ULTRASONIC CONSOLIDATION AS NOVEL MANUFACTURING TECHNIQUE IN EMBEDDING PASSIVE/ACTIVE FIBRES IN METAL MATRICES

M. Amir Siddiq , Elaheh Ghassemieh

Dept. of Mechanical Engineering, University of Sheffield, UK

ABSTRACT

Ultrasonic consolidation process is a rapid manufacturing process used to join thin layers of metal at low temperatures and low energy consumption. In this work, finite element method has been used to simulate the ultrasonic consolidation of Aluminium alloys 6061 (AA-6061) and 3003 (AA-3003). A thermomechanical material model has been developed in the framework of continuum cyclic plasticity theory which takes into account both volume (acoustic softening) and surface (thermal softening due to friction) effects. A friction model based on experimental studies has been developed, which takes into account the dependence of coefficient of friction upon contact pressure, amount of slip, temperature and number of cycles. Using the developed material and friction model ultrasonic consolidation process has been simulated for various combinations of process parameters involved.

Experimental observations are explained on the basis of the results obtained in the present study. The current research provides the opportunity to explain the differences of the behaviour of AA-6061 and AA-3003 during the ultrasonic consolidation process. Finally, trends of the experimentally measured fracture energies of the bonded specimen are compared to the predicted friction work at the weld interface resulted from the simulation at similar process condition. Similarity of the trends indicates the validity of the developed model in its predictive capability of the process.

INTRODUCTION

Ultrasonic consolidation is a rapid manufacturing process in which ultrasonic energy is used to create a solid state bond among different layers of composites, metals and alloys. It is a solid state joining process with low temperature and requires low process energy. Main advantages of ultrasonic consolidation include, absence of liquid-solid transformations, no atmosphere control required, low energy consumption, low temperature allows embedding of electronics, such as sensors and actuators.

Ultrasonic power required to join two components increase as the size (thickness) of the specimens being joined increase. Therefore, this limitation of thickness has restricted its use to microelectronics industry. Typical applications include, metal encased sensors, metal composite shields, fibre reinforced metal/matrix composites, satellite panels, electrical and electronic joints.

A number of researchers [**1, 2, 3, 4, 5, 6**] have performed experimental studies on ultrasonic consolidation process and have reported both surface and volume effects during ultrasonic consolidation process. However, very little effort has been made to develop theoretical models to simulate ultrasonic consolidation process [**7**]. In all the theoretical and simulated works, the effect of ultrasonic vibration is attributed in the friction coefficient rather than taking

into account both surface and volume effects. In the presented work, a material model based on cyclic plasticity theory has been proposed to take into account the volume effects as well as surface effects. Also, a kinematic friction model has been proposed to include the contribution of surface effects during ultrasonic consolidation process.

METHODOLOGY

Finite element analyses of the ultrasonic consolidation process have been performed using coupled temperature-displacement analysis. Material properties of the aluminium alloys (AA-6061 and AA-3003) have been assigned using the proposed material model. The material model is based on the combined nonlinear isotropic/kinematic hardening model for time independent cyclic plasticity presented by Chaboche and coworkers [**8, 9**]. The modified isotropic and kinematic hardening equations are given in Table 1:

Table 1: Modified Chaboche [10, 9] material model with thermal and acoustic softening

Isotropic hardening:	$R = Q\left(1 - e^{-b\bar{\varepsilon}^{pl}}\right)$ where $\bar{\varepsilon}^{pl}$ is the equivalent plastic strain, while Q and b are material parameters to be identified by inverse modelling.
Nonlinear kinematic hardening [**11**]:	$\dot{\underline{\alpha}} = \frac{C}{\gamma}\left(\underline{\sigma} - \underline{\alpha}\right)\dot{\bar{\varepsilon}}^{pl} - \gamma\underline{\alpha}\dot{\bar{\varepsilon}}^{pl}$ where C and γ are the material parameters which can be identified from cyclic testing.
Modified hardening rules with thermal softening:	
Thermomechanical isotropic hardeing law:	$R_{th} = R \cdot \left(1 - \hat{\theta}^{m}\right)$ where m is the material parameter and $\hat{\theta}$ is the nondimensional temperature given as $\hat{\theta} = \frac{\theta - \theta_{transition}}{\theta_{melt} - \theta_{transition}}$ $\theta_{transition}$ is the transition temperature, at or below which there is no temperature dependence on yield stress, and θ_{melt} is the melting temperature.
Thermomechanical nonlinear kinematic hardening law:	$\alpha_{th} = \alpha \cdot \left(1 - \theta^{m}\right)$
Modified hardening rules with acoustic (ultrasonic) softening:	
Isotropic hardening law with acoustic softening:	$R_{ultrasonic} = R_{th} \cdot \left(1 - d \cdot E_{ultrasnonic}\right)^2$
Kinematic hardening law with acoustic softening:	$\alpha_{ultrasonic} = \alpha_{th} \cdot \left(1 - d \cdot E_{ultrasonic}\right)^2$ Where d is ultrasonic softening parameter which has to be identified from experiments of deformation behaviour of the material in the presence of ultrasonic energy.

Parameters for the proposed material model have been identified using inverse modelling technique. The parameters identified are given in Table 2 while comparison of experimental and simulated response is plotted Figure 1.

Table 2: Material parameters obtained by inverse modelling

Material	σ_{y0} (MPa)	Q (MPa)	b	C (GPa)	γ (MPa)	*m*	*d* (m^2/W)
AA-6061	50	100	20.0	15.0	60.0	1.642081	1.3×10^{-6}
AA-3003	190	150	25.0	12.0	500.0	0.7	1.3×10^{-6}

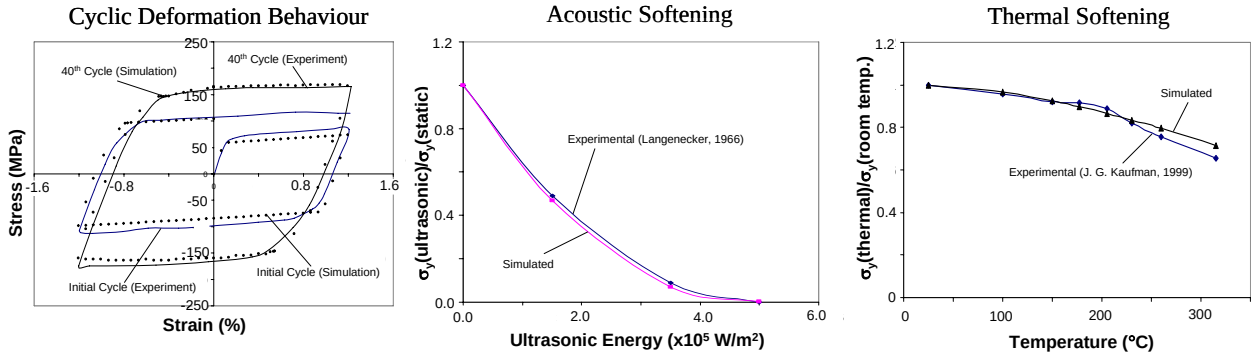

Figure 1: Comparison of experimental and simulated response during parameter identification

Thermomechanical interaction properties at various interfaces are discussed in the following. The normal contact properties at foil/sonotrode, foil/fibre, fibre/substrate, and foil/substrate interfaces are defined using hard contact formulation available in ABAQUS [12]. The friction properties between foil (aluminium alloy) and sonotrode (steel) are defined using pressure dependent isothermal coefficient of friction in coulombs friction model. The friction between foil and substrate is defined using thermomechanical friction model. The friction model proposed in this work is based on the dependence of coefficient of friction μ, on number of cycles *N*, temperature *T*, and parameters *a* and *b* which depend upon magnitude of slip and contact pressure. Friction model is summarized in Table 3. Comparison between experimental friction coefficient and simulated response during identification procedure is plotted in Figure 2.

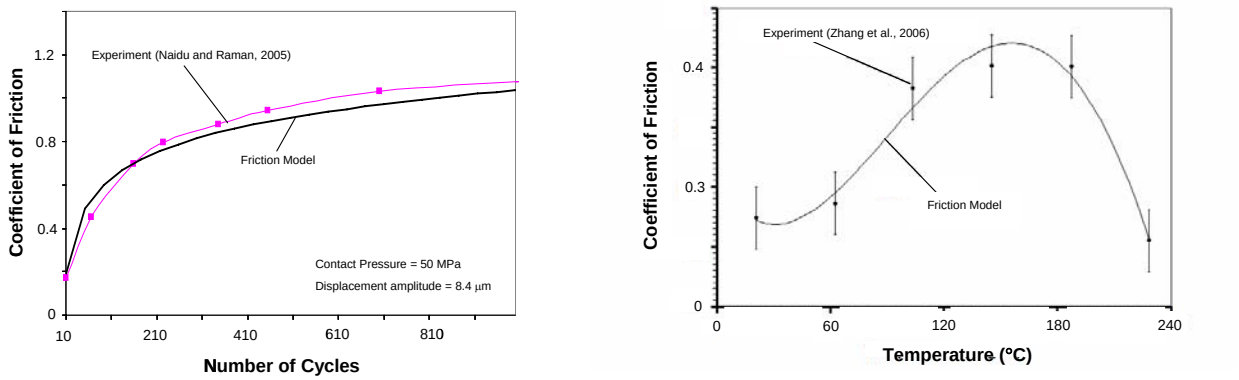

Figure 2: Comparison of experimental and simulated response during parameter identification

Friction properties at foil/fibre and substrate/fibre interfaces are defined using coulomb's friction model with coefficient of friction to be 0.2. Throughout this work it is assumed that all the

friction energy generated between different contacting surfaces is converted into heat energy.

Results of the thermomechanical analyses of the ultrasonic consolidation process for monolithic and fibre embedding specimen have been discussed in the following.

Table 3: Friction model

Isothermal COF:	$\mu_{iso} = \mu_s + \mu_s \cdot (a \cdot \log(N) + b)$ where a and b are friction parameters depend upon the magnitude of the slip amplitude and contact pressure, while μ_s is the initial static coefficient of friction, and N is number of cycles.
Thermomechanical COF:	$\mu = \mu_{iso} \cdot (p \cdot T^4 + q \cdot T^3 + r \cdot T^2 + s \cdot T + t)$ The additional friction parameters p, q, r, s, t are identified using the experimental results [**13**] for aluminium alloy.

DISCUSSION

Monolithic Specimen

Temperature profile during ultrasonic consolidation of monolithic AA-6061 and AA-3003 is plotted in Figure 3. The plot in Figure 3 is only for on set of process parameters; other process parameters were also simulated and found to show similar behaviour. It has been found that maximum temperature at foil/sonotrode interface is highest due to the highest amount of friction dissipation at this interface. It is also found that maximum temperature attained during ultrasonic consolidation process is well below melting temperatures (30-60% of melting temperature). Results also show that temperature in AA-3003 is found to be higher than AA-6061, which is due to the fact that AA-3003 is much harder than AA-6061. It must also be noted that initial yield strength of AA-3003 is approximately 4 times larger than that of AA-6061. Temperature results are also in agreement with the experimental results of Cheng and Li [**14**], where temperature for the case of copper and nickel were found to be in the range of 100-250 ºC at a distance of 200 μm (at Point A in Figure 3) from the weld interface. Similar values of the temperature, with slight variations, are found for other sets of process parameters.

The contour plots of equivalent plastic strain are shown in Figure 4. It is found that regions of the foil near foil/sonotrode interface undergo severe plastic deformation. This high plastic deformation is due to high friction dissipation and ultrasonic energy transferred to the foil near foil/sonotrode interface. It can also be inferred from Figure 4 that amount of plastic deformation in foil near the foil/substrate interface is higher than the plastic deformation in the substrate. This is due to the dual effect, i.e. surface (friction dissipation at the foil/sonotrode and foil/substrate interface) and volume (ultrasonic softening) effects. On the other hand the substrate has the dominating surface effects, i.e. friction dissipation at the foil/substrate interface, and very small amount of volume (acoustic softening) effects to cause plastic deformation. It is also found that plastic strains in AA-6061 at foil/sonotrode interface are almost twice as high as AA-3003, as AA-6061 is 4 time softer than AA-3003. Also, plastic strain at the foil/substrate interface for AA-6061 are lower than AA-3003. This is due to the higher friction work for the case of AA-

3003 which is found to be 10-53 time higher than that of AA-6061 for various combinations of process parameters (see Figure 5).

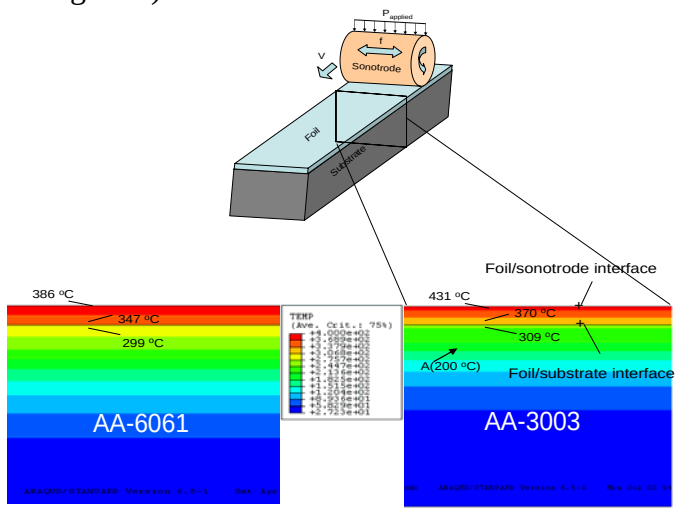

Figure 3: Temperature profile in monolithic specimen (velocity=27.8 mm/sec; Load = 175 MPa; Amplitude = 8.4 μm)

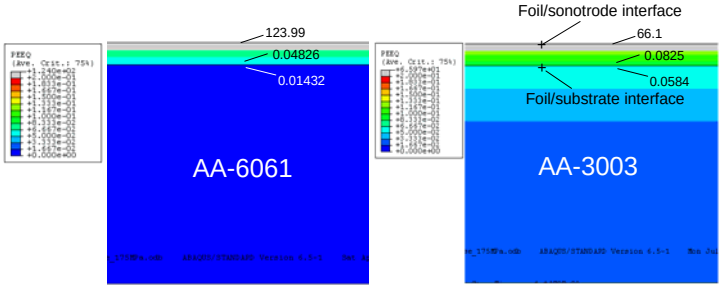

Figure 4: Equivalent plastic strain in substrate and foil at foil/substrate interface (velocity=27.8 mm/sec; Load = 175 MPa; Amplitude = 8.4 μm)

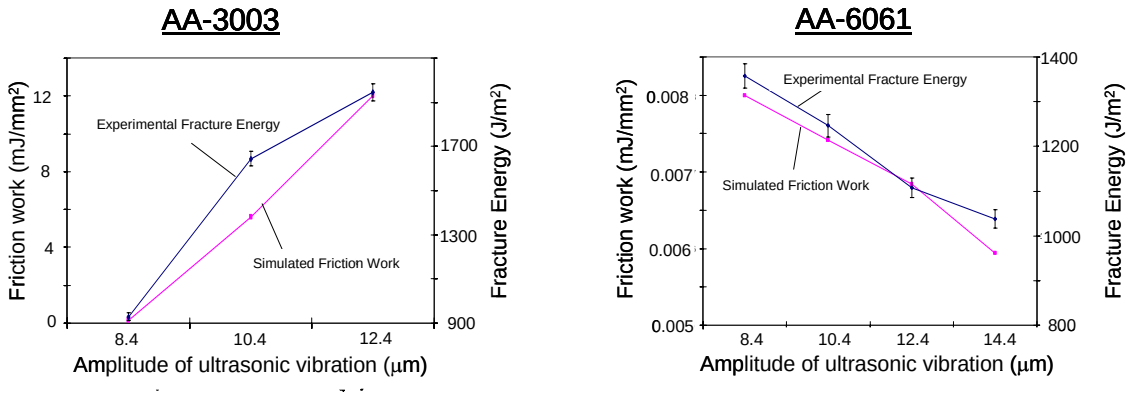

Figure 5: Friction work and experimental fracture energies as a function of amplitude of ultrasonic vibration

A comparison among the friction work at the weld interface and fracture energies computed from peel test curves for both alloys (AA-3003 and AA-6061) has been made in Figure 5. For the case of AA-3003, experimental fracture energies are found to be increasing with increasing amplitude of ultrasonic vibration, similar trends can be seen in Figure 5 (left

figure) for friction work at the weld interface. Simulation results conclude that increase of fracture energy is mainly due to the increasing friction work at the weld interface. The reason for the increase could be understood by considering the fact that as the amount of applied loading is always lower than the static yield stress of AA-3003, the friction dissipation starts well before yielding can occur as a result of applied load and ultrasonic oscillation. Therefore the frictio work for the case of AA-3003 increases with the increasing applied load and amplitude of ultrasonic vibration. On the other hand, experimental fracture energy and friction work show an opposite trend. It can be inferred from Figure 5 (right figure) that experimental fracture energies as well as friction work from simulation decrease with increasing amplitude of ultrasonic vibration. Simulation results conclude that the decrease in friction work causes less breaking off and dispersion of oxide layers, ultimately resulting into smaller number of bonds between the opposing surfaces (weaker joints). The decrease in friction work for the case of AA-6061 is due to the plastic dissipation which starts in less number of ultrasonic cycles. Another important conclusion that can be inferred from Figure 5 that friction work at the weld interface for the case of AA-3003 is higher than that of the AA-6061. This is why AA-6061 required extra cleaning process [**3**] before welding while AA-3003 was successfully welded without any apriori treatment.

Fibre Embedding Specimen

Finite element analyses of Silicon Carbide (SiC) fibre embedding in AA-6061 have been performed using the material and friction models developed in this work. A qualitative comparison of plastic deformation with experimental results is shown in Figure 6. Both simulation and experimental results indicate severe deformation at foil/sonotrode interface during ultrasonic consolidation experiments. It is also found that material flows completely around the firbe as is observed during ultrasonic consolidation experiments. In other words, during experiments [**2, 15**] material showed full closure of voids around the fibre (Figure 6(a)), results of the thermomechanical analyses of ultrasonic consolidation process show the similar effects (Figure 6(b). Maximum plastic deformation in fibre embedding specimen is found to be more than 50 times higher as compared to the monolithic specimens. This is due to the large plastic deformation in the aluminium alloy as a consequence of material flow around the fibre.

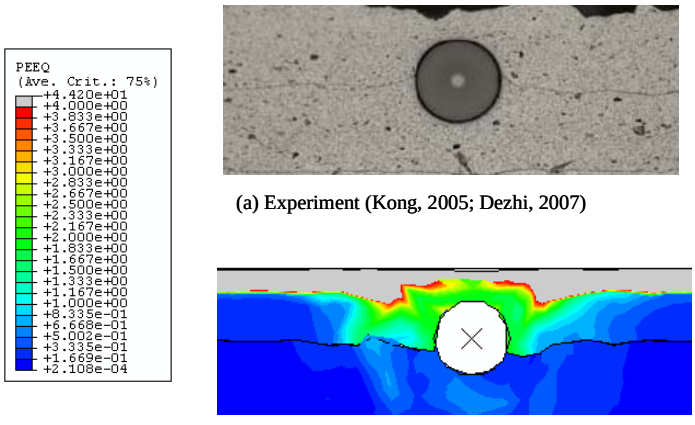

(a) Experiment (Kong, 2005; Dezhi, 2007)

(b) Simulation

Figure 6: Comparison between experimental and simulated material deformation in a UC specimen

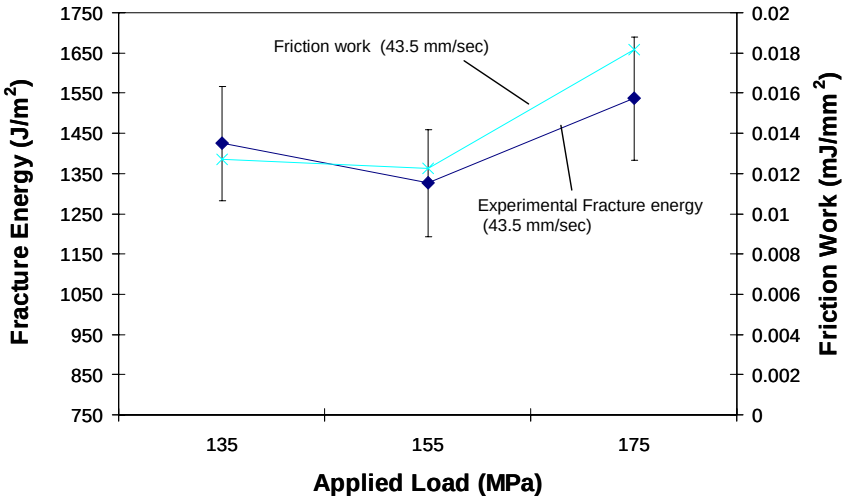

Figure 7: Comparison between experimental fracture energies and simulated friction work for various applied loadings and velocities of sonotrode (displacement amplitude of ultrasonic vibration = 10.4 μm)

A comparison between experimental fracture energies obtained from peel tests and simulated friction work (obtained in the present work) is shown in Figure 7. Results for the case when velocity of sonotrode is 43.5 mm/sec, have been plotted for the cases when displacement amplitude of the ultrasonic vibration was 10.4 μm. Simulated friction works show similar trends as experimentally measured fracture energies [**16**].

CONCLUSIONS

The presented work shows the capability of the developed material and friction model in simulating the ultrasonic consolidation process for monolithic as well as fibre embedding specimen. The results of thermomechanical analyses showed that ultrasonic consolidation of monolithic AA-6061 behaves differently than AA-3003. Maximum temperature is found to be 30-60% of the melting temperature. A comparison of friction work values of AA-6061 and AA-3003 was also made and it is found that friction work of AA-3003 is always higher than the friction work of AA-6061. Comparison of experimental fracture energies and simulated friction works show similar trend for different process parameters.

Thermomechanical analyses results of fibre embedding using ultrasonic consolidation process showed that material flows completely around the fibre as is observed during ultrasonic consolidation experiments. Plastic flow is found to be maximum at foil/sonotrode interface. Comparison of experimental fracture energies and simulated friction work showed similar trends.

ACKNOWLEDGMENTS

The authors thankfully acknowledge the financial support of EPSRC (Engineering and Physical Sciences Research Council) and MOD (Ministry of Defence) through the grant (GR/T19988) and the collaborative support of the Solidica Ltd.

REFERENCES

1. K. C. Joshi, *The formation of ultrasonic bonds between metals*, Welding Journal **50** (1971), 840-848.
2. C. Y. Kong, "Investigation of ultrasonic consolidation for embedding active/passive fibres in aluminium matrices," *Rapid Manufacturing Center*, vol. PhD, Loughborough University, Loughborough, UK, 2005, pp. 1-207.
3. C. Y. Kong, R. C. Soar and P. M. Dickens, *Characterisation of aluminium alloy 6061 for the ultrasonic consolidation process*, Materials Science and Engineering A **360** (2003), 99-106.
4. ---, *Optimum process parameters for ultrasonic consolidation of 3003 aluminium*, Journal of Materials Processing Technology **146** (2004), 181-187.
5. J. E. Krzanowski, *A transmission electron microscopy study of ultrasonic wire bonding*, IEEE Trans. CHMT **13** (1990), 176-181.
6. J. C. Tucker, "Ultrasonic welding of copper to laminate circuit board," *Materials Science & Engineering*, vol. MSc, Worcester Polytechnic Institute, 2002, p. 125.
7. C. Doumanidis and Y. Gao, *Mechanical modelling of ultrasonic welding*, Welding Journal **4** (2004), 140-146.
8. J. L. Chaboche, *Time independent constitutive theories for cyclic plasticity*, International Journal of Plasticity **5** (1986), 247-302.
9. ---, *Constitutive equations for cyclic plasticity and cyclic viscoplasticity*, International Journal of Plasticity **5** (1989), 247-302.
10. ---, *Viscoplastic constitutive equations for the description of cyclic and anisotropic behaviour of metals*, De l✗Acad. Polonaaise des Sciences, Sevie Sc. Et Techn **25** (1977), no. 33.
11. P. J. Armstrong and C. O. Frederick, "A mathematical representation of the multiaxial bauschinger effect," CEGB Report No. RD/B/N 731, 1966.
12. ABAQUS, "Abaqus version 6.5, online documentation," Hibbit & Karlsson, 2006.
13. C. B. Zhang, X. J. Zhu and L. J. Li, "A study of friction behaviour in ultrasonic welding (consolidation) of aluminium.," *AWS Conference: Session 7: Friction and resistance welding/materials bonding processes*, 2006.
14. X. Cheng and X. Li, *Investigation of heat generation in ultrasonic metal welding using micro sensor arrays*, J. Micromechanics and microengineering **17** (2007), no. 2, 273-282.
15. D. Li, "Report for machine performance validation through comparison of peel strength and linear weld density of samples made before and after machine maintenance," Rapid Manufacturing Research Group, Loughborough University, Loughborough, 2007, pp. 1-14.
16. ---, "Defining optimum parameters for embedding sic fibres and influence on bond strength in al 6061 matrix," Rapid Manufacturing Research Group, Loughborough University, Loughborough, UK, 2007, pp. 1-19.